Journal of Power Sources 183 (2008) 749–754

Contents lists available at ScienceDirect

Journal of Power Sources

journal homepage: www.elsevier.com/locate/jpowsour

Structural stability of chemically delithiated layered $(1-z)Li[Li_{1/3}Mn_{2/3}]O_2$–$zLi[Mn_{0.5-y}Ni_{0.5-y}Co_{2y}]O_2$ solid solution cathodes

Y. Wu, A. Manthiram*

Electrochemical Energy Laboratory & Materials Science and Engineering Program, The University of Texas at Austin, Austin, TX 78712, United States

ARTICLE INFO

Article history:
Received 9 April 2008
Received in revised form 7 May 2008
Accepted 8 May 2008
Available online 17 May 2008

Keywords:
Lithium ion batteries
Layered oxide cathodes
Chemical delithiation
Structural stability

ABSTRACT

Lithium has been chemically extracted from the layered oxide solid solutions $Li[Li_{1/3}Mn_{2/3}]O_2$–$(z)Li[Mn_{0.5-y}Ni_{0.5-y}Co_{2y}]O_2$ ($0 \le y \le 1/2$ and $0.25 \le z \le 0.75$) and characterized by X-ray diffraction. The weak super lattice reflections that occur in the parent samples at around $2\theta = 20$–25° vanish on extracting a significant amount of lithium due to the removal of lithium from the transition metal layer and a consequent loss of the ordering between the Li^+ and the transition metal ions. Additionally, the chemical delithiation process results in an incorporation of some protons from the chemical delithiation medium into the layered lattice, which has an influence on the structure of the delithiated samples. While the incorporation of a higher concentration (~0.4 per formula unit) of protons results in the formation of O1 or P3 phases, delithiated samples with <0.2 protons maintain the initial O3 structure. However, the electrochemically charged samples maintain the initial O3 structure.

1. Introduction

Layered oxide solid solutions between $Li[Li_{1/3}Mn_{2/3}]O_2$ (commonly designated as Li_2MnO_3) and $LiMO_2$ ($M = Mn_{0.5}Ni_{0.5}$ [1–5], Co [6], and Cr [7,8]) have become appealing as promising cathode materials for lithium ion batteries due to their high reversible capacity of around 250 mAh g^{-1} with a lower cost and better safety compared to the currently used $LiCoO_2$ cathode. Although these solid solutions have the O3 structure similar to the $LiCoO_2$ cathode, they exhibit superstructure reflections arising from an ordering of Li^+ and Mn^{4+} ions as they have a large charge difference [9]. While Li_2MnO_3 is electrochemically inactive as it is difficult to oxidize beyond Mn^{4+}, its solid solutions with other $LiMO_2$ oxides have been found to exhibit good electrochemical activity. The higher capacities of these solid solutions are due to the irreversible loss of oxygen from the lattice during the first charge [10,11] and a lowering of the oxidation state of the transition metal ions at the end of first discharge compared to the oxidation state value in the initial material.

Delmas et al. [12] classified the layered alkali metal oxides A_xMO_2 into various types of structure such as O1, O3, P2, P3, T2, and T1, in which the letters O (octahedral), P (prismatic), and T (tetrahedral) refer to the coordination environment of the alkali metal ion, and the number 1–3 refer to the number of MO_2 sheets per unit cell. The $LiMO_2$ cathodes such as $LiCoO_2$ adopt the O3 structure shown in Fig. 1(a), which has an oxygen stacking sequence of . . .ABCABC. . . along the *c*-axis. During the lithium extraction (charging) process, the MO_2 sheets can slide, yielding O1 type (space group: $P\bar{3}m1$) or P3 type (space group $R3m$) structures that have an oxygen stacking sequences of, respectively, . . .ABABAB. . . and . . .AABBCC. . . along the *c*-axis as shown in Fig. 1(b) and (c) [13,14]. Such phase transformations during charging can have a profound influence on the reversibility of the lithium extraction process and consequently the reversible capacity values of the layered oxide cathodes.

Our group has been focusing on the chemical and structural instabilities of the layered $Li_{1-x}MO_2$ ($0 \le x \le 1$) oxides that were obtained by chemically extracting lithium with NO_2BF_4 in acetonitrile medium, and the results have shown that the chemically delithiated layered oxides exhibit significant differences in structure depending on their initial composition and the nature of the transition metal ions present [14–20]. We present here a systematic investigation of the structural evolution of the chemically delithiated $(1-z)Li[Li_{1/3}Mn_{2/3}]O_2$–$(z)Li[Mn_{0.5-y}Ni_{0.5-y}Co_{2y}]O_2$ ($0 \le y \le 1/2$ and $0.25 \le z \le 0.75$) solid solution series. The type of phases formed on chemical delithiation is correlated to the proton content inserted into the layered lattice from the chemical delithiation medium.

2. Experimental

All the samples presented in this study were synthesized by a coprecipitation method in which required amounts of the transition metal acetates were dissolved in deionized water and then

* Corresponding author. Tel.: +1 512 471 1791; fax: +1 512 471 7681.
E-mail address: rmanth@mail.utexas.edu (A. Manthiram).

0378-7753/$ – see front matter © 2008 Elsevier B.V. All rights reserved.
doi:10.1016/j.jpowsour.2008.05.028

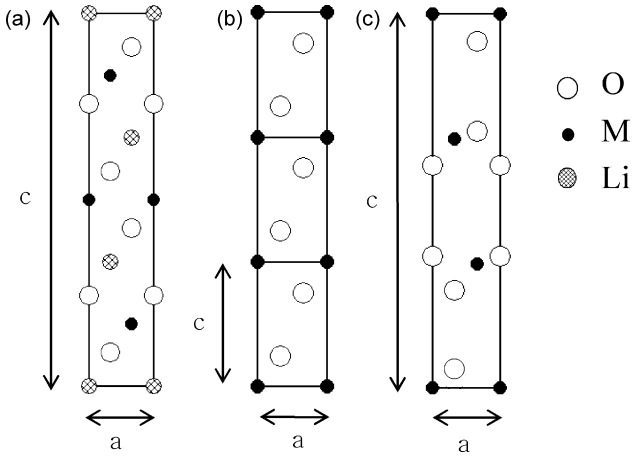

Fig. 1. Crystal structures of (a) O3 type $LiMO_2$, (b) O1 type MO_2, and (c) P3 type MO_2 viewed along the (1 0 0) plane.

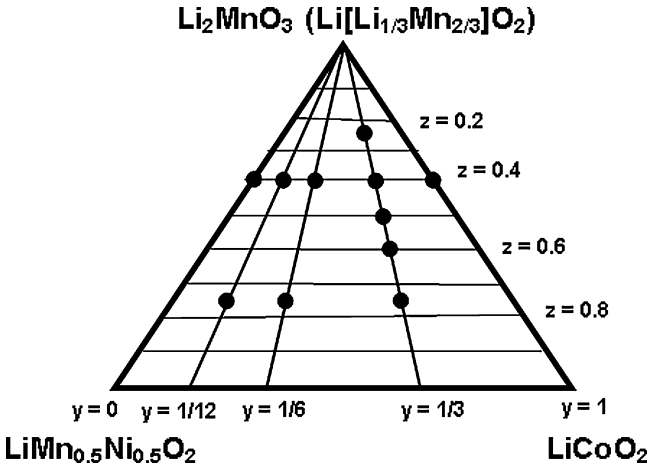

Fig. 2. Compositional phase diagram of the $(1-z)Li[Li_{1/3}Mn_{2/3}]O_2$–$(z)Li[Mn_{0.5-y}Ni_{0.5-y}Co_{2y}]O_2$ $(0 \le y \le 0.5$ and $0.25 \le z \le 0.75)$ solid solution series.

added drop by drop into a 0.1-M KOH solution to form the coprecipitated hydroxides of Mn, Co, and Ni. After drying overnight at 100 °C in an air-oven, the coprecipitated hydroxides were mixed with a required amount of lithium hydroxide, fired in air at 900 °C for 24 h, and then quenched into liquid nitrogen. Chemical extraction of lithium was carried out by stirring 1.0 g of the synthesized oxide powder with 30 mL of an acetonitrile solution of the oxidizer NO_2BF_4 for 2 days under an argon atmosphere, followed by washing the products with acetonitrile using an Schlenk line. The amount of NO_2BF_4 in the reaction mixture was about 25% more than that required based on the reaction below:

$$LiMO_2 + NO_2BF_4 \rightarrow Li_{1-x}MO_2 + xNO_2 + xLiBF_4 \quad (1)$$

All the products were characterized by X-ray diffraction with Cu Kα radiation. Structural refinements and lattice parameter determinations were carried out by analyzing the X-ray diffraction data with the Rietveld method using the DBWS-9411 PC program [21]. Lithium contents in the synthesized and delithiated samples were determined by atomic absorption spectroscopy (AAS). The average oxidation state of the transition metal ions present in the samples was determined by treating the samples with a known excess of sodium oxalate and titrating the unreacted sodium oxalate with potassium permanganate. Our previous study has shown that chemical delithiation of layered oxides with NO_2BF_4 often results in an ion exchange of some Li^+ ions by H^+ ions that could be produced by an oxidation of acetonitrile by the powerful oxidizer NO_2BF_4 during chemical delithiation [14,22]. Accordingly, the proton contents in the delithiated samples were determined by prompt gamma-ray activation analysis (PGAA) by irradiating the samples for 2 h at a reactor power of 950 kW as described elsewhere [22].

Electrochemical performances were evaluated with CR2032 coin cells at a current density of 12.5 mA g^{-1} (~C/20 rate) between 4.8 V and 2.0 V. Cathodes were prepared by mixing 75 wt.% active material with 20 wt.% acetylene black and 5 wt.% PTFE binder, rolling the mixture into thin sheets of about 0.1-mm thick, and cutting into circular electrodes of 0.64 cm^2 area; CR2032 coin cells were then assembled with the cathodes thus fabricated, lithium anode, and 1 M $LiPF_6$ in ethylene carbonate (EC)/diethyl carbonate (DEC) electrolyte, and Celgard polypropylene separator.

3. Results and discussion

The compositions studied in the $(1-z)Li[Li_{1/3}Mn_{2/3}]O_2$–$(z)Li[Mn_{0.5-y}Ni_{0.5-y}Co_{2y}]O_2$ $(0 \le y \le 1/2$ and $0.25 \le z \le 0.75)$ solid solution series are indicated by closed circles in Fig. 2, and the observed compositions based on the experimentally determined lithium contents and the average oxidation state of the transition metal ions for the parent materials are listed in Table 1. The X-ray diffraction data indicated all the samples to be single-phase materials belonging to the layered O3 structure shown in Fig. 1(a). For example, the X-ray diffraction patterns of the $(1-z)Li[Li_{1/3}Mn_{2/3}]O_2$–$(z)Li[Mn_{0.5-y}Ni_{0.5-y}Co_{2y}]O_2$ $(0 \le y \le 1/2$ and $z = 0.4)$ series of samples (i.e. $Li[Li_{0.2}Mn_{2(1.5-y)/5}Ni_{2(0.5-y)/5}Co_{4y/5}]O_2$ with $0 \le y \le 1/2)$ are given in Fig. 3(a). In addition to the reflections corresponding to the O3 layered structure, weak superstructure reflections were observed around $2\theta = 20$–$25°$, which are known to correspond to the ordering of the Li^+ and transition metal ions in the transition metal layer of the layered lattice [9]. For all the samples in the $z = 0.4$ series (i.e. $Li[Li_{0.2}Mn_{2(1.5-y)/5}Ni_{2(0.5-y)/5}Co_{4y/5}]O_2$ with $0 \le y \le 1/2$), the lithium content value in the transition metal layer remains the same as 0.2, but the intensities of the superlattice peaks decrease with increasing value of y or increasing Co content as seen in Fig. 3(a). This change is due to the relatively high concentration of Co^{3+} ions that disturbs the clustering of the Mn^{4+} and Ni^{2+} around the lithium ions in the transition metal layers [23]. The variations of the lattice parameters a and c with y in $0.6Li[Li_{1/3}Mn_{2/3}]O_2$–$0.4Li[Mn_{0.5-y}Ni_{0.5-y}Co_{2y}]O_2$ (i.e. $Li[Li_{0.2}Mn_{2(1.5-y)/5}Ni_{2(0.5-y)/5}Co_{4y/5}]O_2$ with $0 \le y \le 1/2$) are shown in Fig. 3(b). Both the lattice parameters decrease monotonically with increasing y-value due to an increasing replacement of the larger Ni^{2+} (0.069 nm) ions by the smaller Co^{3+} ions (0.0545 nm), illustrating the formation of solid solutions. The c/a ratio increases from 4.980 at $y = 0$ to 4.998 at $y = 1/3$, which is in good agreement with the trend reported for the $Li[Mn_{0.5-y}Ni_{0.5-y}Co_{2y}]O_2$ samples [24].

Fig. 4 shows the XRD patterns of the fully delithiated samples in the $z = 0.4$ series that were obtained by chemically extracting lithium from the parent samples with NO_2BF_4 in acetonitrile. The data reveal that all the delithiated samples maintain the O3 structure similar to the parent lithiated sample. The Rietveld fitting shown in Fig. 5(a) for the delithiated sample with $z = 0.4$ and $y = 1/6$ shows good matching between the observed and calculated O3 patterns with a satisfactory goodness of fit $s = 2.07$ and a low R_{wp} value of 12.70%. A close comparison of the XRD patterns in Fig. 4 and those in Fig. 3(a) reveals that the superlattice reflections present in the parent samples vanish after chemically extracting most of the lithium. With an aim to determine the lithium content at which the superlattice reflections disappear, we chemically extracted dif-

Table 1
Chemical analysis data of the chemically delithiated $(1-z)Li[Li_{1/3}Mn_{2/3}]O_2$–$(z)Li[Mn_{0.5-y}Ni_{0.5-y}Co_{2y}]O_2$ samples

z	y	Observed parent composition	Observed composition after chemical delithiation	Structure after delithiation	% cation disorder
	0	$Li[Li_{0.2}Mn_{0.6}Ni_{0.2}]O_2$	$H_{0.17}Li_{0.18}[Li_{0.2}Mn_{0.6}Ni_{0.2}]O_{1.72}$	O3	3.9
	1/12	$Li[Li_{0.2}Mn_{0.56}Co_{0.07}Ni_{0.17}]O_2$	$H_{0.16}Li_{0.21}[Li_{0.2}Mn_{0.56}Co_{0.07}Ni_{0.17}]O_{1.79}$	O3	3.1
0.4	1/6	$Li[Li_{0.2}Mn_{0.54}Co_{0.13}Ni_{0.13}]O_2$	$H_{0.14}Li_{0.16}[Li_{0.2}Mn_{0.54}Co_{0.13}Ni_{0.13}]O_{1.74}$	O3	2.5
	1/3	$Li[Li_{0.2}Mn_{0.47}Co_{0.27}Ni_{0.06}]O_2$	$H_{0.06}Li_{0.12}[Li_{0.2}Mn_{0.47}Co_{0.27}Ni_{0.06}]O_{1.61}$	O3	0.9
	1/2	$Li[Li_{0.2}Mn_{0.4}Co_{0.4}]O_2$	$H_{0.16}Li_{0.12}[Li_{0.2}Mn_{0.4}Co_{0.4}]O_{1.64}$	O3	0.8
0.25		$Li[Li_{0.25}Mn_{0.54}Ni_{0.04}Co_{0.17}]O_2$	$H_{0.13}Li_{0.19}[Li_{0.25}Mn0_{.54}Co_{0.17}Ni_{0.04}]O_{1.75}$	O3	0.3
0.4		$Li[Li_{0.2}Mn_{0.47}Ni_{0.06}Co_{0.27}]O_2$	$H_{0.06}Li_{0.12}[Li_{0.2}Mn_{0.47}Co_{0.27}Ni_{0.06}]O_{1.61}$	O3	0.9
0.5	1/3	$Li[Li_{0.16}Mn_{0.43}Ni_{0.08}Co_{0.33}]O_2$	$H_{0.11}Li_{0.05}[Li_{0.16}Mn_{0.42}Co_{0.33}Ni_{0.08}]O_{1.61}$	O3	0
0.6		$Li[Li_{0.13}Mn_{0.37}Ni_{0.1}Co_{0.4}]O_2$	$H_{0.19}Li_{0.01}[Li_{0.13}Mn_{0.37}Co_{0.4}Ni_{0.1}]O_{1.73}$	O3	0.7
0.75		$Li[Li_{0.08}Mn_{0.29}Ni_{0.13}Co_{0.5}]O_2$	$H_{0.42}[Li_{0.08}Mn_{0.29}Co_{0.5}Ni_{0.13}]O_{1.82}$	O3 + P3	0
	1/12	$Li[Li_{0.08}Mn_{0.48}Co_{0.13}Ni_{0.31}]O_2$	$H_{0.36}Li_{0.01}[Li_{0.08}Mn_{0.48}Co_{0.13}Ni_{0.31}]O_{1.83}$	O3 + O1	1.5
0.75	1/6	$Li[Li_{0.08}Mn_{0.42}Co_{0.25}Ni_{0.25}]O_2$	$H_{0.42}[Li_{0.08}Mn_{0.42}Co_{0.25}Ni_{0.25}]O_{1.83}$	O3 + O1	1.1
	1/3	$Li[Li_{0.08}Mn_{0.29}Ni_{0.13}Co_{0.5}]O_2$	$H_{0.42}[Li_{0.08}Mn_{0.29}Co_{0.5}Ni_{0.13}]O_{1.82}$	O3 + P3	0

ferent amounts of lithium from the parent samples and examined the XRD patterns as shown in Fig. 6 for the $z = 0.4$ series. In Fig. 6, x refers to the amount of lithium extracted from the parent samples. As seen in Fig. 6, the intensity of the superstructure reflections around $2\theta = 20$–25° decreases with an increasing amount of lithium extracted (denoted as x in Fig. 6), and the superstructure reflections are hard to observe for $x > 0.6$. In the $z = 0.4$ series of samples that can be represented as $Li[Li_{0.2}M_{0.8}]O_2$ (M = Mn, Ni, and Co) for simplicity, the extraction of about 0.4 lithium ions corresponds to the oxidation of the transition metal ions to 4+ state, and further extraction of lithium ions is accompanied by an irreversible loss of oxygen from the layered lattice. Based on solid state NMR studies [25], the depletion of lithium ions from the lithium layer has been suggested to be compensated by a migration of lithium ions from the transition metal plane to the lithium plane, which results in a disturbance of the cation ordering in the transition metal plane and a consequent vanishing of the superstructure reflections.

Fig. 7 shows the variations of the lattice parameters with the amount of lithium extracted (x) from the parent material for the $z = 0.4$ series with $y = 0$, 1/12, 1/3, and 1/6. The a parameter decreases initially with increasing x due to an increase in the oxidation state of the transition metal ions and then tend to become nearly constant as the oxidation state of the transition metal ions remain constant although oxide ions are being lost from the lattice and small amounts of protons are inserted into the lattice from the chemical delithiation medium as seen in Table 1. The c parame-

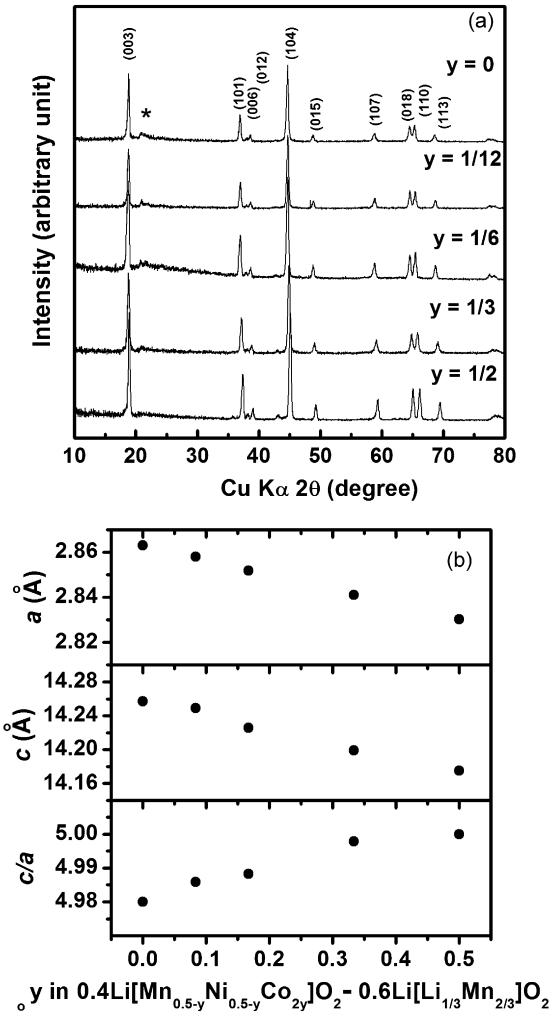

Fig. 3. (a) XRD patterns of the $(1-z)Li[Li_{1/3}Mn_{2/3}]O_2$–$(z)Li[Mn_{0.5-y}Ni_{0.5-y}Co_{2y}]O_2$ ($z = 0.4$ and $0 \le y \le 0.5$) samples and (b) variations of the lattice parameters a and c, and c/a ratio with y in the $z = 0.4$ series.

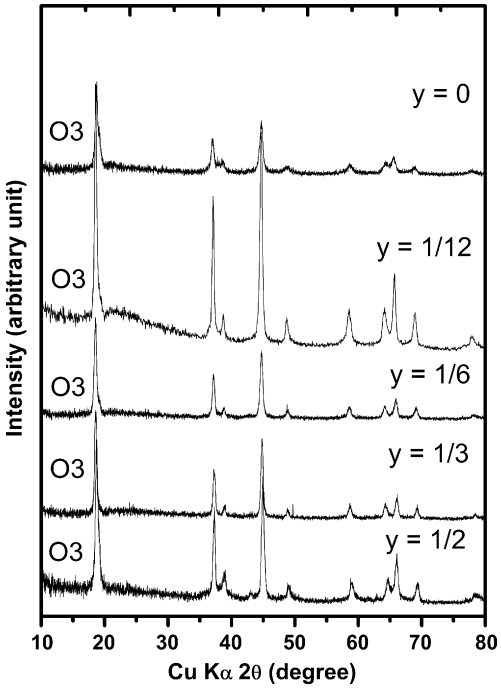

Fig. 4. XRD patterns of the fully delithiated samples that were obtained from the $(1-z)Li[Li_{1/3}Mn_{2/3}]O_2$–$(z)Li[Mn_{0.5-y}Ni_{0.5-y}Co_{2y}]O_2$ ($z = 0.4$ and $0 \le y \le 0.5$) series of samples by reacting them with NO_2BF_4 in acetonitrile.

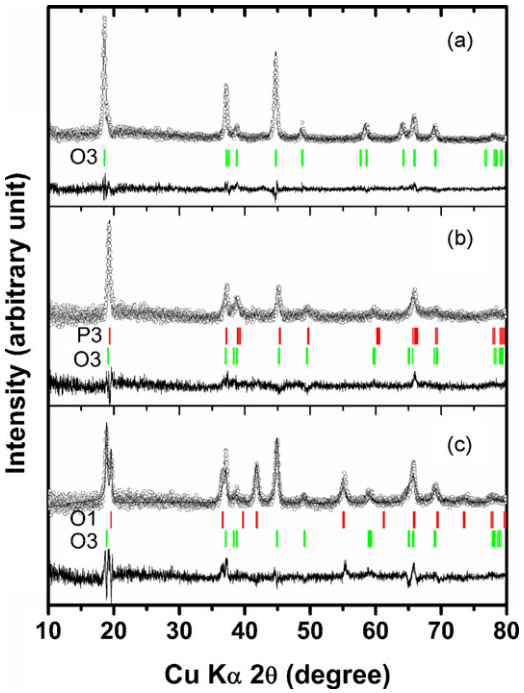

Fig. 5. Rietveld fitting of the XRD data of the chemically delithiated samples obtained from the $(1-z)Li[Li_{1/3}Mn_{2/3}]O_2$–$(z)Li[Mn_{0.5-y}Ni_{0.5-y}Co_{2y}]O_2$ series of samples: (a) $y = 1/6$ and $z = 0.4$ sample that has $s = 2.07$ and $R_{wp} = 12.70\%$, (b) $y = 1/3$ and $z = 0.75$ sample that has $s = 2.15$ and $R_{wp} = 14.33\%$, and (c) $y = 1/12$ and $z = 0.75$ sample that has $s = 2.44$ and $R_{wp} = 14.87\%$.

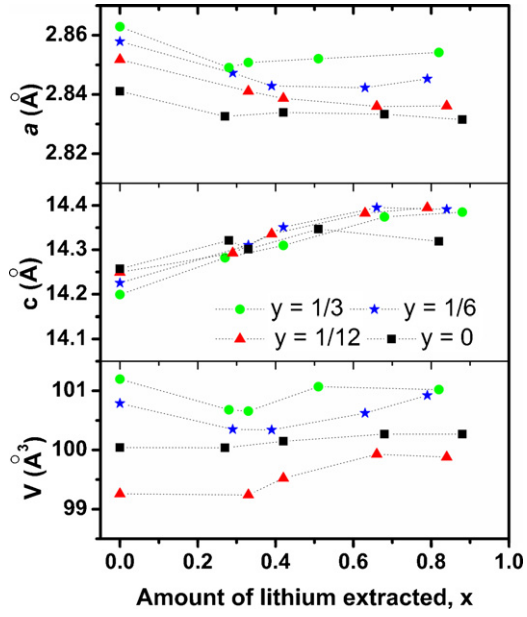

Fig. 7. Variation of the lattice parameters with the amount of lithium extracted (x) chemically from the $(1-z)Li[Li_{1/3}Mn_{2/3}]O_2$–$(z)Li[Mn_{0.5-y}Ni_{0.5-y}Co_{2y}]O_2$ ($z = 0.4$ and $0 \le y \le 0.5$) series of samples.

ter increases initially with the amount of lithium extracted (x) due to an increasing electrostatic repulsion across the van der Waals gap between the MO_2 (M = Mn, Ni, and Co) sheets and then tends to become nearly constant due to the loss of oxygen from the lattice and an insertion of small amounts of protons. These opposite trends in the initial variations of a and c lattice parameters result in a very small overall volume change (<1%) with lithium extraction x.

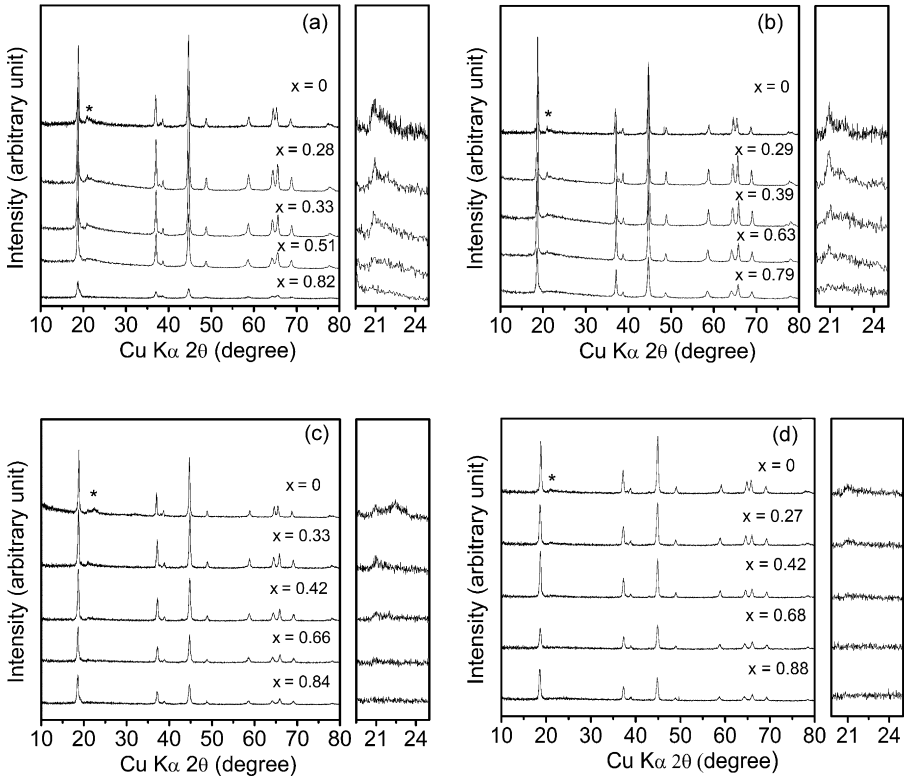

Fig. 6. XRD patterns of the delithiated samples that were obtained by extracting different amounts of lithium (x) from the $(1-z)Li[Li_{1/3}Mn_{2/3}]O_2$–$(z)Li[Mn_{0.5-y}Ni_{0.5-y}Co_{2y}]O_2$ ($z = 0.4$ and $0 \le y \le 0.5$) series of samples: (a) $y = 0$, (b) $y = 1/12$, (c) $y = 1/6$, and (d) $y = 1/3$. The insets on the right show an expanded view of the patterns over a small 2θ range.

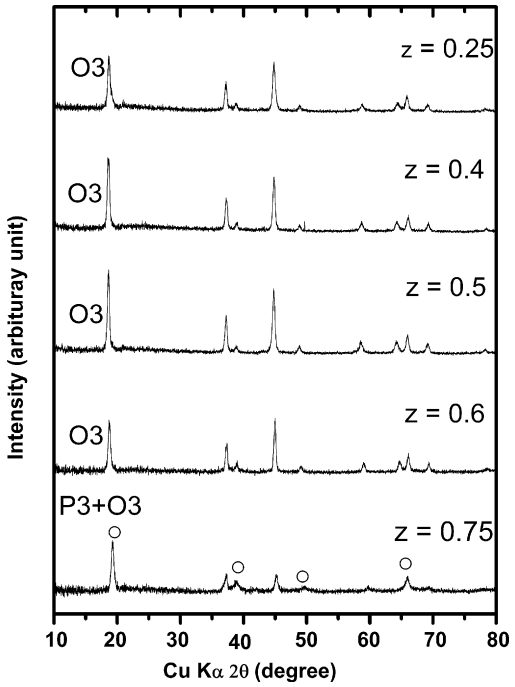

Fig. 8. XRD patterns of the fully delithiated samples that were obtained from the $(1-z)Li[Li_{1/3}Mn_{2/3}]O_2$–$(z)Li[Mn_{0.5-y}Ni_{0.5-y}Co_{2y}]O_2$ ($y = 1/3$ and $0 \le z \le 0.75$) series of samples by reacting them with NO_2BF_4 in acetonitrile. The unmarked reflections refer to the O3 phase while the reflections marked with (◯) refers to the P3 phase.

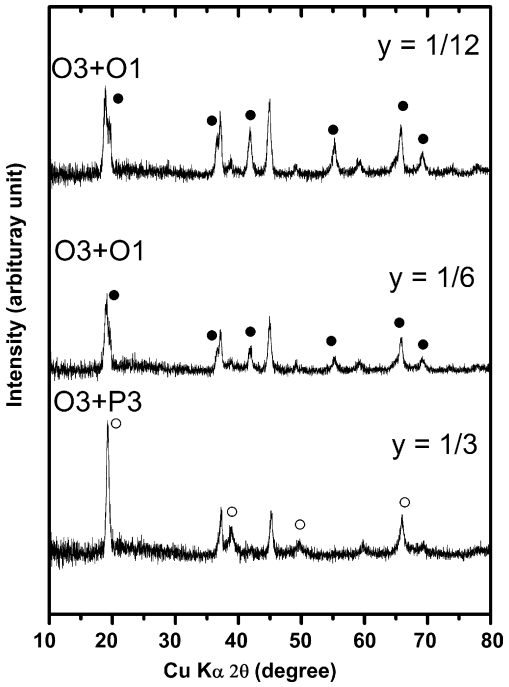

Fig. 9. XRD patterns of the fully delithiated samples that were obtained from the $(1-z)Li[Li_{1/3}Mn_{2/3}]O_2$–$(z)Li[Mn_{0.5-y}Ni_{0.5-y}Co_{2y}]O_2$ ($y = 1/12$, 1/6, and 1/3 and $z = 0.75$) series of samples by reacting them with NO_2BF_4 in acetonitrile. The unmarked reflections refer to the O3 phase while those marked with (◯) and (●) refer, respectively, to the P3 and O1 phases.

Fig. 8 shows the XRD patterns of the delithiated samples for the $y = 1/3$ and $0.25 \le z \le 0.75$ series. While the delithiated samples maintain the initial O3 structure for $z \le 0.6$, the $z = 0.75$ sample shows the formation of a P3 phase in addition to the initial O3 structure as indicated by the open circles in Fig. 8. Rietveld refinement indicated the P3 phase to be about 35%, and the fitting result is shown in Fig. 5(b) with a satisfactory goodness of fit $s = 2.15$ and $R_{wp} = 14.33\%$. For the samples with $y = 1/12$, 1/6, and 1/3 and $z = 0.75$, the delithiated samples all showed a mixture of the initial O3 structure and a new P3 (open circles) or O1 (solid circles) phase as seen in Fig. 9. The Rietveld fitting result shown in Fig. 5(c) for the $y = 1/12$ and $z = 0.75$ sample reveal the formation of a new O1 phase with a satisfactory goodness of fit $s = 2.44$ and $R_{wp} = 14.87\%$.

Combining the results from atomic absorption for lithium content analysis, redox titration for oxidation state analysis, and PGAA for proton content determination, Table 1 gives the compositions of the chemically delithiated samples. All the delithiated samples contain some residual lithium and inserted protons with a significant amount of oxygen loss from the lattice. For simplicity, the lithium contents in the transition metal layer for the chemically delithiated materials are kept the same as that in the parent sample although it has been suggested in the literature that the lithium ions migrate from the transition metal layer to the lithium layer. The % cation disorder in the parent sample arising from a small difference in the ionic radii of Ni^{2+} (0.69 Å) and Li^+ (0.76 Å) is also given in Table 1. Generally, a high cation disorder prevents the sliding of the MO_2 sheets and the formation of P3 or O1 phases from the initial O3 phase [19] as the polyhedra (octahedra or prism) in the lithium plane share both edges and faces with the MO_6 octahedra in the transition metal plane in the O1 and P3 structures and the presence of any M^{n+} ions in the lithium plane will exert strong electrostatic repulsion across the shared polyhedral faces in the O1 and P3 structures unlike in the O3 structure that has only edge sharing between the octahedra in the lithium plane and transition metal plane.

As the samples in this study do not have a high cation disorder as seen in Table 1, especially for samples with $y = 1/3$ and $0.25 \le z \le 0.75$, no clear relation is found between the degree of cation disorder and the type of phases formed for the delithiated samples. On the other hand, the amount of proton inserted from the chemical delithiation medium into the layered lattice seems to play a significant role in the type of phases formed. For example, the delithiated samples with $z = 0.75$ and $y = 1/12$, 1/6 and 1/3 containing a high concentration of protons (~0.4 per formula unit) encounter the formation of O1 or P3 phases, while those containing a low concentration of protons (<0.2 per formula unit) maintain the initial O3 structure. An ion exchange of the Li^+ ions by the H^+ ions generated by the oxidation of acetonitrile by the strong oxidizer NO_2BF_4 used in chemical delithiation favors the gliding of the MO_2 sheets due to the hydrogen bonding stabilization provided by the P3 structure [26,27]. Although the reason for the formation of P3 versus O1 phase is not clear here, previous studies have attributed the formation of metastable P3 phase to a faster lithium extraction rate due to good cation ordering or larger surface area of the layered oxide samples, while a slow lithium extraction leads to the formation of the thermodynamically more stable O1 phase [14].

However, no significant insertion of protons is expected during the electrochemical delithiation (charging). To delineate the differences between the chemical delithiation and the electrochemical charging processes, the $y = 1/3$ and $z = 0.75$ cathode material was charged to 4.8 V at both $C/20$ and $2C$ rates and the XRD patterns of the electrochemically charged sample is compared with that of the chemically delithiated sample in Fig. 10. The $y = 1/3$ and $z = 0.75$ sample maintains the parent O3 structure after electrochemically charging at both $C/20$ and $2C$ rate in contrast to the P3 phase formation for the chemically delithiated sample. The data thus demonstrate that the formation of P3 or O1 phases for the chemically delithiated samples is largely due to the insertion of a significant amount of protons into the layered lattice and the

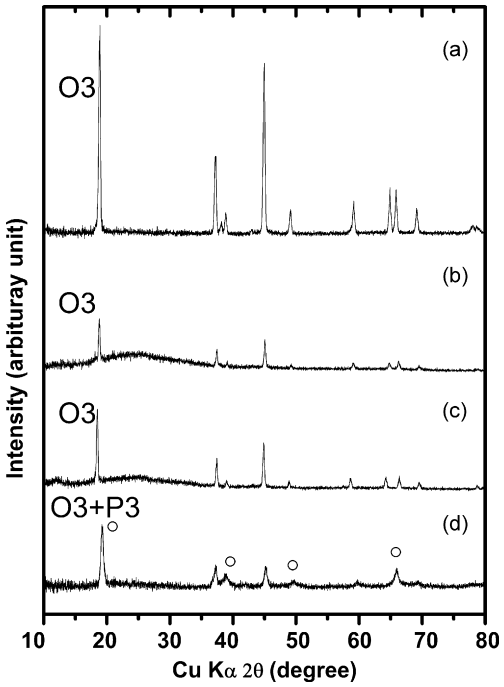

Fig. 10. Comparison of the XRD patterns of the electrochemically charged and chemically delithiated samples obtained from the $(1-z)Li[Li_{1/3}Mn_{2/3}]O_2$–$(z)Li[Mn_{0.5-y}Ni_{0.5-y}Co_{2y}]O_2$ ($y=1/3$ and $z=0.75$) series of samples: (a) parent undelithiated sample, (b) sample charged electrochemically to 4.8 V at C/20 rate, (c) sample charged electrochemically to 4.8 V at 2*C* rate, and (d) $H_{0.42}Li_{0.08}Mn_{0.29}Co_{0.5}Ni_{0.13}O_{1.82}$ obtained by chemical delithiation. The unmarked reflections refer to the O3 phase while the reflections marked with (◯) refers to the P3 phase.

consequent stability imparted by the hydrogen bonding to the P3 phase.

4. Conclusions

The structural stability of the layered $(1-x)Li[Li_{1/3}Mn_{2/3}]O_2$–$(z)Li[Mn_{0.5-y}Ni_{0.5-y}Co_{2y}]O_2$ ($0 \le y \le 0.5$ and $0.25 \le z \le 0.75$) solid solution samples on extracting lithium chemically from them has been investigated. The superlattice reflections arising from an ordering of the Li^+ and transition metal ions vanish in all the samples on extracting more than 0.6 lithium per formula unit. Also, delithiated samples that have ~0.4 protons incorporated from the chemical delithiation medium tend to transform to P3 or O1 structures, while those with <0.2 protons maintain the initial O3 structure similar to the O3 phase found with the electrochemically charged samples.

Acknowledgments

Financial support by NASA through the Houston Advanced Research Center (HARC) and the Welch Foundation Grant F-1254 is gratefully acknowledged.

References

[1] Z. Lu, L.Y. Beaulieu, R.A. Donaberger, C.L. Thomas, J.R. Dahn, J. Electrochem. Soc. 149 (2002) A778.
[2] S.H. Kang, Y.K. Sun, K. Amine, Electrochem. Solid State Lett. 6 (2003) A183.
[3] Y.J. Park, Y.S. Hong, X. Wu, K.S. R, S.H. Chang, J. Power Sources 129 (2004) 288.
[4] S.H. Kang, K. Amine, J. Power Sources 124 (2003) 533.
[5] D.A.R. Barkhouse, J.R. Dahn, J. Electrochem. Soc. 152 (2005) A746.
[6] J. Jiang, K.W. Eberman, L.J. Krause, J.R. Dahn, J. Electrochem. Soc. 152 (2005) A1879.
[7] L. Zhang, H. Noguchi, J. Electrochem. Soc. 150 (2003) A601.
[8] B. Ammundsen, J. Paulsen, I. Davidson, J. Electrochem. Soc. 149 (2002) A431.
[9] Z. Lu, Z. Chen, J.R. Dahn, Chem. Mater. 15 (2003) 3214.
[10] Z.H. Lu, J.R. Dahn, J. Electrochem. Soc. 149 (2002) A815.
[11] R. Armstrong, M. Holzapfel, P. Novak, C.S. Johnson, S.-H. Kang, M.M. Thackeray, P.G. Bruce, J. Am. Chem. Soc. 128 (2006) 8694.
[12] C. Delmas, P. Fouassier, Hagenmuller, Physica B 99 (1980) 81.
[13] M. Butel, L. Gautier, C. Delmas, Solid State Ionics 122 (1999) 271.
[14] J. Choi, A. Manthiram, J. Mater. Chem. 16 (2006) 1726.
[15] R.V. Chebaim, F. Prado, A. Manthiram, Chem. Mater. 13 (2001) 2951.
[16] S. Venkatraman, Y. Shin, A. Manthiram, Electrochem. Solid State Lett. 6 (2003) A9.
[17] S. Venkatraman, A. Manthiram, Chem. Mater. 14 (2002) 3907.
[18] R.V. Chebaim, F. Proado, A. Manthiram, J. Solid State Chem. 163 (2002) 5.
[19] S. Venkatraman, A. Manthiram, Solid State Ionics 176 (2005) 291.
[20] J. Choi, A. Manthiram, J. Electrochem. Soc. 152 (2005) A1714.
[21] R.A. Young, The Rietveld Method, Oxford University Press, New York, 1993.
[22] J. Choi, E. Alvarez, T.A. Arunkumar, A. Manthiram, Electrochem. Solid State Lett. 9 (2006) A241.
[23] S.H. Kang, P. Kempgen, S. Greenbaum, A.J. Kropf, K. Amine, M.M. Thackeray, J. Mater. Chem. 17 (2007) 2069.
[24] J. Choi, A. Manthiram, Solid State Ionics 176 (2005) 2251.
[25] C.P. Grey, W.S. Yoon, J. Reed, G. Ceder, Electrochem. Solid State Lett. 7 (9) (2004) A290.
[26] Y. Paik, C.P. Grey, C.S. Johnson, J.S. Kim, M.M. Thackeray, Chem. Mater. 14 (2002) 5109.
[27] A.D. Robertson, P.G. Bruce, Chem. Mater. 15 (2003) 1984.